RESONANT CIRCUIT DESIGN PROCEDURE FOR MULTI-WATT T5 ELECTRONIC BALLASTS

M. S. Perdigão[(1), (3)], A. R. Seidel[(2)], H. V. Marques[(1)], J. M. Alonso[(4)], and E. S. Saraiva[(1)]
(1) Instituto de Telecomunicações, DEEC, Universidade de Coimbra Pólo II, P-3030-290 Coimbra, Portugal
(2) Universidade Federal de Santa Maria, GEDRE, GSEC, Santa Maria, RS, 97105-900, Brasil
(3) IPC, Instituto Superior de Engenharia de Coimbra, DEE, R. Pedro Nunes, 3030-199 Coimbra, Portugal
(4) Universidad de Oviedo, Electrical & Electronics Eng. Dept., 33204-Gijón, Asturias, Spain
perdigao@isec.pt, esaraiva@deec.uc.pt, marcos@uniovi.es, seidel@ctism.ufsm.br

***Abstract* – This paper proposes a resonant circuit design procedure for multi-Watt magnetically-controlled electronic ballasts. The procedure is focused on the ballast performance, which has the advantage of operating at constant-frequency, and complies with current IEC standards (IEC 60081) regarding nominal lamp operation, namely electrode safe operation. Data collected from T5 tubular fluorescents lamps manufacturers and the Sum of Squares (SoS) technique are both used to define the suitable design methodology for the power range of the selected T5 lamps. Experimental results for a set of T5 fluorescent lamps are presented in order to validate the entire design procedure.**

***Keywords* - Electronic Ballasts, Fluorescent Lamps, Resonant Converters, Magnetic Control, Multi-Watt Electronic Ballast, Power Electronics.**

I. INTRODUCTION

The application of magnetic control in dimmable electronic ballasts and universal or multi-Watt electronic ballast was recently proposed as a viable and efficient solution for fluorescent lighting [1]-[5]. This control technique is based on a simple premise: controlling the circuit through the variation of the resonant frequency, instead of varying the inverter operating frequency. The technique is implemented by means of a dc-controlled magnetic element, the magnetic regulator. Several published papers show a variety of possible applications for the magnetic regulator in its various forms: variable inductor or transformer. The device can be used in LED drivers [6], as reactive power compensator in electrical power systems [7], for dynamic load impedance correction in induction heaters [8], and to eventually provide ZVS or ZCS operation in dc-dc converters [9].

A key issue when developing electronic ballasts (EB) for tubular fluorescent lamps (FLs) is to evaluate the physical conditions of the fluorescent lamp (FL) electrodes during the lamp operation since, as stated in [10], the lifetime of a FL is determined by the electrode operation. In order to ensure sufficient electrode lifetime, its temperature should be kept within certain limits. Above a certain temperature the electrodes will be too hot, leading to enhanced evaporation of the emissive material and severe end-blackening. Below a certain temperature the electrodes will be too cold and sputtering of the emitter will occur. Both situations may lead to an extremely short lamp life. This implies that, tubular FLs will obviously present restrictions that must be taken into account in the design of any EB. Thus, more than just applying traditionally well-known EB design procedures, in terms of resonant filters [11]-[31], it is also necessary to evaluate the electrode operating conditions under those.

One way to evaluate the conditions for proper and safe operation of the electrodes is based on the sum of squares of the lead-in wire currents (SoS). These limits are based in the maximum permissible currents that may pass through the electrodes. In 2006 these limits were still under discussion at the European Lamp Manufacturers Association for the Preparing of Standards, but, in due time, it was expected that they would result in new data in the relevant IEC standards [10]. These limits are now referred to in the IEC 60081 international standard (recent edition 2010) [32], [33]. Up to the present time only few works consider the electrode proper operation in the design of the resonant filter in EB [26]-[31], [33]. Among them, only [29], [31] and [33] consider the SoS limits as evaluation method for both electrode operation and EB resonant filter design, primarily in dimming conditions.

The research presented in this paper shows a magnetic electronic ballast capable of operating high efficiency and high output (HO) T5 FLs. This research is mainly focused on pointing out critical issues related to the electrode operation, regulations, FL features, and the SoS approach which is taken into account in order to define a suitable design methodology for the high frequency multi-Watt operation [32].

In terms of tubular FL technology, T5 are considered the state of the art. When compared to T8, they present a 40% smaller diameter. The material reduction due to miniaturization makes them environmental friendly and contributes also to the reduction of manufacturing costs.

Compared to T8 and T12 FLs, T5 are specially characterized by a high lamp voltage, and in some particular cases, low current. This is the reason why they are conventionally manufactured for HF operation, typically above 20 kHz. Since maximum efficiency is only attained with HF operation, 50/60 Hz operation is usually not recommended. Nevertheless, some authors have recently investigated the use of low-frequency low-loss magnetic ballasts. The main argument is the fact that there will be an

Manuscript received on 18/10/2012. Revised on 16/01/2013. Accepted for publication in 16/01/2013 to Special Session by recommendation for the Special Editors Ricardo Nederson do Prado e Pedro Francisco Donoso-García.

obvious public health consequence due to electronic waste accumulation in the environment, with other adverse impacts such as soil and water pollution. In [34] it is suggested the control of T5 28W lamps, which are the common replacement of T8 36W lamps, with ultra-low LC magnetic ballasts. Evidences show the possibility to ignite and operate the T5 28W lamp at low frequency, with very small consequences in the lamp efficacy. The fact is that there is an obvious advantage which is inherent to the low-current feature of this lamp, which also enables a significant reduction in both conductions and core losses in the magnetic ballast.

Therefore, it is possible, that in special circumstances, magnetic ballasts may stand as a correct choice. But, on the other hand, multi-Watt operation, remote control and most importantly, control of the electrode operation conditions are automatically discarded.

In this paper, Section II describes the standard multi-Watt EB topology with magnetic control and T5 HE/HO operation limits according to standards and manufacturers data, considering safe electrode operation. Section III presents the standard design procedure regarding parameter estimation and points out the possible impact of this procedure on the electrodes operation. It also describes typical conditions for obtaining ZVS operation. A new design procedure based on the SoS limits which guarantees proper electrode operation is proposed. Theoretical predictions are compared to experimental results for a range of 14W-49W T5 HE, HO Philips FLs, with a special attention to the electrodes currents are presented in Section IV. Finally, Section V presents main conclusions regarding this proposed design methodology.

II. MULTI-WATT BALLAST WITH SAFE ELECTRODE OPERATION

A. T5 HE/HO Multi-Watt Ballast

The schematic of a standard multi-Watt magnetically-controlled electronic ballast (MCEB) is presented in Figure 1. This type of ballast uses a parallel-loaded high frequency (HF) half-bridge inverter. Two additional blocks are required: the magnetic regulator, which replaces the typical resonant inductor, and the dc current source, to control this regulator. The regulator operates as a variable inductance as response to the dc control current, I_{dc}. A higher value of I_{dc} corresponds to a lower value of the inductance L_{ac}.

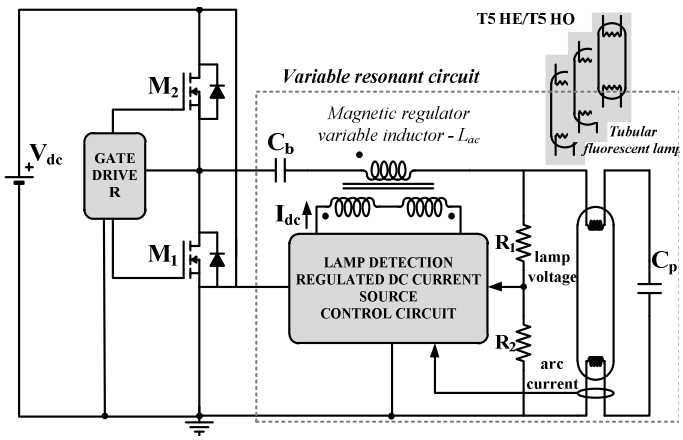

Fig. 1. Standard multi-Watt EB circuit with magnetic control.

By simply controlling the magnetic device an adaptable and flexible resonant circuit is provided. Hence, a simple and effective control method is used which avoids typical control methods for universal operation: adapting V_{dc} or simultaneously change both switching frequency and duty-ratio of the inverter signal.

The ability to change and adapt the resonant circuit to the working parameters imposed by each lamp is consequently integrated in the ballast. Opposed to other commercial ballasts, MCEB may be operated at constant-frequency, which is an important advantage since it reduces the switching losses and electromagnetic interference stresses. In this control technique the parallel capacitor value, C_p remains constant. The power delivered to each selected FL can be adjusted according to its wattage rate, by simply changing the filter characteristics [1]-[5].

Developing an appropriate design methodology for the resonant circuit parameters, guaranteeing proper lamp operation, including safe ignition and correct electrode temperature are essential to the ballast project.

B. Electrode Operation - SoS Limits

1) General considerations - Presently, there are several regulations regarding ballast and luminaire design. Issues regarding installation, environment, performance, operation conditions, ignition and electrodes pre-heating are referred to in several IEC standards [32], [35], [36].

The ignition process is a decisive factor in terms of electrode preservation with an immediate effect on the lamp life. Repeated lamp switching evidently shortens the lamp life and these are the reasons why the pre-heating process is extremely important to ensure a longer lamp life.

For similar reasons as well as to avoid evaporation of the emissive material, it is also extremely important to maintain the electrodes temperature at an appropriate level during normal or dimming FL operation [37]. Obviously, all of these issues are critical aspects to be considered while developing a new highly efficient MCEB. As will be described, the proposed multi-Watt MCEB will provide soft-starting and correct electrode temperature for all FLs in nominal operation. The developed design methodology will show that it is possible to overcome eventual critical points related to electrode operation. The existence of these critical points affects the FL life and negatively contributes to the performance of whole system.

2) Soft-starting and pre-heating - For the parallel loaded MCEB shown in Figure 1, the usual method for soft-starting the FL is to control the inverter switching frequency, f_s [14]. The frequency is reduced until the starting voltage is obtained, igniting the FL. By employing magnetic regulators, it is possible to use the variable ac inductance as additional control parameter to achieve soft-starting in a narrower frequency range similarly as the switching frequency method. This process may be observed in Figure 2.

Firstly, the inverter frequency is set at the selected value. Secondly, the dc current is adjusted in order to get the maximum inductance value, L_{ph}. During this operation the electrodes are pre-heated due to the current that flows into the parallel capacitor, before the ignition of the FL. Afterwards, the value of the inductance is lowered to L_{ig}, by

increasing the dc control current, until the FL is ignited. Then, the inductance must be set at the appropriate level, L_{ac}, according to the selected FL. This action may easily be accomplished by the microcontroller (μC) and must be done respecting the pre-heating times, defined for each FL by the manufacturer. Other soft-starting processes may involve electrode pre-heating from external heating sources (North America practice), in rapid-start circuits or warm-start circuits [36], [38].

3) SoS limits - According to IEC standards, the proper method to evaluate the electrodes operating conditions is based on the SoS limits. Thus, in order to prevent the decrease of FL life, these limits which are imposed by T5 FL manufacturers should always apply. The SoS definition shown in (1) takes into account both electrodes currents, as defined in Figure 3. In Figure 3.a I_{res}, represents the resonant current, I_D the discharge current, I_H the heating current, I_{LH} the higher lead wire current and finally I_{LL} the lower lead wire current. Figure 3.a I_H is flowing through the entire electrode by entering via one electrode lead-in wire and leaving by the other and it is equal to I_{LL}. Therefore, measuring the current through one of the lead-in wires will result in a value for I_H, while the other will represent the superposition of I_D and I_H which will correspond to the total current I_{LH} [39] as it can be represented in Figure 3.b. These currents are all rms values. For each rated lamp power, maximum rms limit values are defined for each of these currents, for nominal power operation or dimming operation. The electrodes are designed in such a way that the I_D can be varied around its rated value within certain limits without negative impact on the lamp.

$$SoS = {I_{LH}}^2 + {I_{LL}}^2, \qquad I_{LH} > I_{LL} \tag{1}$$

The normal operation is therefore bounded by the minimum and maximum discharge current, I_{Dmin} and I_{Dmax} values. Within these limits of the lamp current, additional heating is not strictly required.

However, I_H has to be limited by a maximum value, in order to prevent strong evaporation of the emissive materials.

This limitation of I_H is necessary for the entire range of I_D. If the lamp current is to be dimmed over a broader range, it may be necessary to supply additional heating to the electrodes to maintain its optimum temperature.

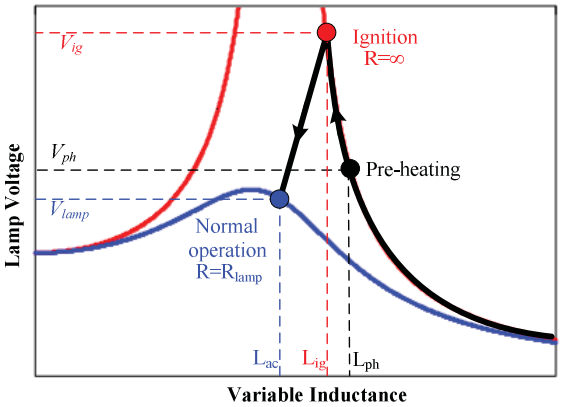

Fig. 2. Soft-starting process using the inductance as control parameter.

This additional heating is only necessary to keep the cathode at a sufficiently high temperature for thermionic emission especially for low current values. If the ballast does include external heating sources, the currents in the lead-in wires I_{LH} and I_{LL} should also be kept below the maximum values, I_{LHmax} and I_{LLmax}, given in the IEC 60081. Therefore I_{LH} has a lower limit to ensure sufficient electrode heating by I_H if the lamp is dimmed whereas in the nominal operation region, the lower boundary for I_H is dictated by the requirement I_{Dmin} [39]. The value of the required additional heating current is a function of I_D (arc current), but it is also dependent on the ballast circuit configuration. For the parallel-loaded circuit shown in Figure 3.a there is an obvious phase-shift between these two currents. However, the research which led to this SoS approach showed a linear dependency between the sum of the squared lead currents to the electrode and the discharge current, where neither the phase shift between I_D and I_H, nor the distribution of the discharge current trough the leads, has an influence [39], [40]. This linear dependence establishes current boundary limits related to the SoS value. Therefore, in dimming operation, instead of having one SoS value for each FL, maximum, minimum and target SoS curves are defined for the whole dimming range. These current boundary limits are defined in (2).

$$\begin{cases} SoS_{min} = X_1 - Y_1 \cdot I_D \\ SoS_{max} = X_2 - Y_2 \cdot I_D \\ SoS_{target} = X_1 - z \cdot Y_1 \cdot I_D \end{cases} \tag{2}$$

The minimum sum of squares, SoS_{min}, is defined to keep the electrode just at a sufficient temperature to prevent cathode sputtering, and the maximum sum of squares, SoS_{max}, is defined to avoid electrode overheating and accelerated end-blackening. In some applications, these boundaries may still be critical in terms of FL performance, so a target and safe SoS line is also defined, SoS_{target}. X_1, X_2, Y_1, Y_2 and z are quantities defined by the manufacturers according to each lamp. For T5 HE FLs, which have the same rated nominal current, these boundaries are the same whatever the lamp wattage. In some other ballast circuits where the additional heating current is delivered by separate heating sources, it is not clear through which lead-in wire will flow part of the lamp current. Nevertheless, whatever the configuration, all these effects can be taken into account by measuring the currents through the two lead-in wires to the electrode and calculating the sum of the squares of these two currents as a function of the discharge current. If this definition is applied to the standard configuration for MCEB, it becomes clear that $I_{res} = I_{LH}$ and $I_H = I_{LL}$.

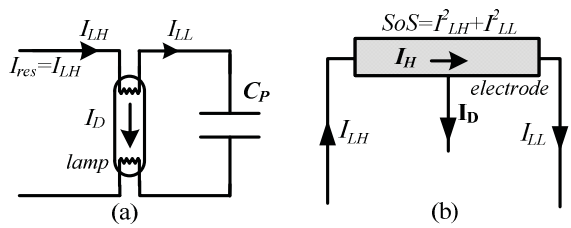

Fig. 3. Currents definition nomenclature for the SoS approach for: (a) Circuit (b) Electrodes.

Lighting engineers involved in standards preparation consider this definition the simplest and most unambiguous way to describe the requirements for proper electrode operation and therefore this technique will be effective when designing the filter circuit. The purpose of this paper is to present an adequate design methodology for the calculation of the filter parameters for a multi-Watt MCEB. The ballast is capable of supplying a broad range of T5 HE and HO FLs at nominal power and at constant f_s. This methodology guarantees that each FL *SoS* limits are respected by limiting the currents to the maximum values established by the IEC standard.

III. MULTI-WATT MCEB DESIGN METHODOLOGY

A. Standard Design Procedure

1) Parameter estimation - The primary goal is to operate all selected lamps (T5 HE series, T5 HO 24W, 39W and 49W) at nominal power while maintaining the same switching frequency, f_s and the same resonant circuit capacitance. Therefore, it is necessary to calculate this capacitance and the inductance value required by each lamp in order to provide universal operation. The circuit is characterized as a low-pass resonant filter and the standard design procedure, using the fundamental-harmonic approximation is adopted [14]. For the half-bridge inverter connected to a parallel-loaded resonant circuit, it can be observed that $\left|\underline{G}(j\omega)\right| = Q_L$ when $f_s/f_o = 1$. In other words, the voltage gain can be approximated by Q at the natural frequency, f_o, Q being the quality factor of the load, as represented in (3). This equation can be used to calculate the base impedance of each resonant circuit, Z_b, for each lamp, using the nominal values for the lamp voltage, V_{lamp}, and the lamp resistance, R_{lamp}. So, as first step, the estimation of the resonant filter parameters, L_{ac} and C_p, is done considering that $f_s = f_o$, using (3)-(5).

$$Q = \frac{V_{lamp}}{V_{rms1}} = \frac{R_{lamp}}{Z_b}; \quad \text{for } f_s = f_o = \frac{1}{2\pi\sqrt{LC_P}} \tag{3}$$

$$Z_b = \sqrt{\frac{L_{ac}}{C_p}}; \quad \text{for } f_s = f_o \tag{4}$$

$$L_{ac} = \frac{Z_b}{2\pi f_o}; \quad C_P = \frac{1}{2\pi Z_b f_o} \tag{5}$$

where $V_{rms1} = \frac{\sqrt{2}}{\pi} V_{dc}$ is the rms value of the fundamental component of the half-bridge output. If the circuit is operated at $f_s = f_o$, the rms value of the discharge for each lamp can be defined as in (6). In these conditions, the circuit will behave as a current source and this current value will depend exclusively on the bridge output voltage and Z_b.

$$I_D = \frac{V_{lamp}}{R_{lamp}} = \frac{V_{rms1} Q}{R_{lamp}} = \frac{V_{rms1}}{Z_b} \tag{6}$$

By taking (6) into consideration, and by using the nominal arc current values for each FL given by the manufacturer, (5) can be rewritten as in (7), and (8). Table I summarizes the determined component values for each T5 FL considering a constant operating frequency, f_s=55kHz, and V_{rms1}=140V for a dc bus voltage V_{dc}= 310V.

$$L_{ac} = \frac{V_{rms1}}{2\pi f_s I_D} \tag{7}$$

$$C_P = \frac{I_D}{2\pi f_s V_{rms1}} \tag{8}$$

TABLE I
Resonant Filter Parameters for T5 Lamps

Lamp	C_b [µF]	C_P [nF]	L_{ac} [mH]
TL5 HE series (14/21/28/35)	1	3.48	2.35
TL5 HO24W	1	6.15	1.33
TL5 HO39W	1	6.94	1.17
TL5 HO49W	1	5.33	1.53

As expected and according to Table I, the resonant capacitor C_P is different for each attached lamp. However, the nature of the desired universal operation requires a different design procedure. For this control technique, it is necessary to determine a single $C_P$value, to operate all T5 FLs considering the determined respective inductances. As initial approach and through the analysis of Table I, an intermediate C_P value is specified. A reasonable option is to set C_P around 4.7 nF, since it is the nearest commercial value for all the selected T5 lamps. Using (9) it is possible to plot the lamp power using the specified resonant parameters and the lamp resistance value. It is important to remind that the lamp resistance is power dependent, $R_{lamp}(P)$. A small change in the lamp power P will have an immediate effect on the resistance value. A recent model even includes temperature effects on the lamp [41]. Figure 4 shows the lamp power behaviour for different FLs, for C_P = 4.7nF. It is observed that for most of the selected lamps a small change in the value of the parallel capacitor will not have a significant effect in the FL power, even if the inductance value is maintained.

$$P = \frac{V_{lamp}^2}{R_{lamp}(P)} = \frac{V_{rms1}^2 R_{lamp}(P)}{R_{lamp}^2(P)(1-\omega^2 L_{ac} C_P) + (\omega L_{ac})^2} \tag{9}$$

The question arising now is how to comply with the referred standard *SoS* limit values and simultaneously identify a maximum limit value for C_P common to all resonant circuits and to guarantee that with this value the ignition of the FL is not compromised.

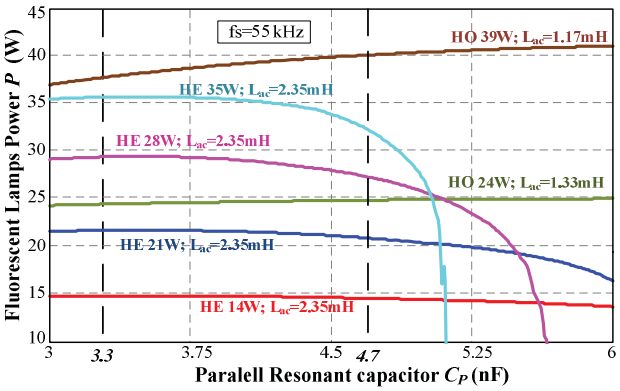

Fig. 4. FLs power P versus parallel capacitor C_P using their respective L_{ac} values.

The following sections will describe the additional steps included into the resonant circuit design methodology to guarantee proper operating conditions. The design methodology considers that no external heating sources are linked to the electrodes.

2) Conditions for obtaining ZVS operation - As key condition for ZVS in the half-bridge switches, the phase shift between the resonant current and the inverter square-wave voltage must be negative. However a more thorough analysis can be easily done by reporting to the classic design methodology. In order to guarantee ZVS operation, the traditional design procedure considers as sufficient condition to operate the half-bridge inverter at a frequency f_s above the resonant frequency of the filter. For the parallel-loaded half-bridge inverter, if the quality factor of the load, Q, defined in (3), is equal or greater than 1, and if the switching frequency, $f_s > f_r$, the circuit is defined as a resonant circuit and will behave as an inductive load. In these conditions, this resonant frequency, f_r, is defined as in (10).

$$f_r = f_o\sqrt{1-\frac{1}{Q^2}}, \qquad Q \geq 1 \tag{10}$$

However, if Q is smaller than 1, the resonant frequency does not exist and the circuit is only characterized as an inductive circuit whatever the switching frequency. The filter current waveform will not be fully sinusoidal and the rule that establishes f_s higher than f_r to obtain ZVS is simply invalid [15]. Still, in both circumstances the inductive characteristic of the circuit guarantees ZVS operation for the half-bridge inverter.

B. Design Procedure Based on the SoS Limits

1) Capacitance selection - The first additional step is to check if the value of C_P defined in section *A* maintains the electrodes operating in a safe mode, using the limit values for the currents I_{LL} and I_{LH} as defined by the IEC 60081.

Figure 5 shows a typical FL model which considers the electrodes resistance, r_e, evenly distributed, as defined in [25]. In FL EB, the impedance of the capacitor C_P is normally very high compared to the value of r_e, so, the maximum C_P can be evaluated considering r_e=0. In this case, the capacitor voltage, V_{C_P} , can be considered equal to the FL voltage. The lamp voltage can be defined as in (11).

$$\left|\underline{V}_{lamp}\right| = \left|\underline{I}_{LL}\right| \cdot \left|\frac{1}{j\omega_s C_p} + r_e\right| \tag{11}$$

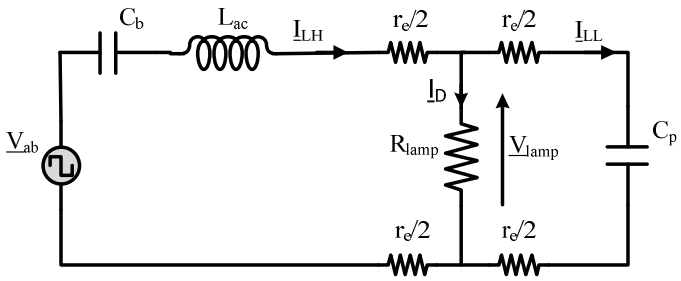

Fig. 5. Conventional equivalent resonant filter circuit.

Taking into consideration that $1/\omega_s C_P \gg r_e$, the maximum capacitance value for each TL5 can be determined by (12), using the limit value for I_{LL} and the V_{lamp} modulus for each lamp (both rms values), according to the data provided by the manufacturer and the IEC 60081 [10].

$$C_P = \frac{\left|\underline{I}_{LL}\right|}{\left|\underline{V}_{lamp}\right| \cdot 2\pi f_s} \tag{12}$$

Table II shows the maximum defined limits for I_{LL}, and I_{LH} and the corresponding maximum allowed C_P value in the filter circuit, obtained from (12), for each T5 FL. The first restriction is set by the T5 HE 35 W lamp. Since this is the FL with the highest lamp voltage, V_{lamp} (and the lowest discharge current, I_D), it will automatically dictate the value of C_P, which will be the lowest value among all, 2.37nF. Capacitance values higher than 2.37nF would damage or reduce the lifetime of this lamp, since the electrodes would be submitted to excessive current, beyond the maximum limit established for I_{LL} and therefore excessive heating.

TABLE II
Nominal and Safety Operation Conditions from TL5 Philips Lamps at 25 °C

Lamp	I_D [mA]	V_{lamp} [V]	I_{LLmax} [mA]	I_{LHmax} [mA]	r_e [Ω]	C_{Pmax} [nF]
HE 14 W	170±40	83 ±10	170	240	40	5.82
HE 21 W	170±40	125 ±10	170	240	40	4.00
HE 28 W	170±40	166 ±17	170	240	40	2.96
HE 35 W	170±40	208 ±20	170	240	40	2.37
HO 24 W	300±30	80 ±8	370	475	12	13.38
HO 39 W	340±70	119 ±10	370	475	12	9.13
HO 49 W	260±50	195 ±20	275	370	16.5	4.07

On the other hand, the analysis of Table II shows that the T5 HO 24 W could allow using capacitance values higher than 12nF without deterioration of the electrodes. However, the proposed control technique requires using a single capacitor for all lamps. The standard resonant circuit design procedure sets a C_P value around 4.7 nF, yet, it is clear now that a lower C_P value must be used in order to operate all lamps in a safe condition: C_P must not exceed 2.37nF. This limit value absolutely guarantees not exceeding the maximum permissible value for I_{LL} for the 35 W FL and therefore the other limit values for the remaining FLs, are implicitly respected.

2) Dual-parallel-capacitor configuration - The nearest commercial value to $C_P = 2.37$nF is 2.2nF. However, it is possible that such a low value does not guarantee a proper ignition for all the lamps, nor that each lamp is even capable of delivering the rated power. Ensuring these conditions represents the next steps of the methodology. A possible solution which simultaneously limits the current I_{LL} and ensures proper lamp operation is to use two parallel resonant capacitors instead of using a single C_P. The capacitor C_P is therefore replaced by capacitors C_{P1} and C_{P2} connected as shown in Figure 6.a. During ignition, these two capacitors will act as a single equivalent resonant capacitor circuit, thereby guaranteeing a higher ignition voltage spike. Thus, with this configuration it is possible to reduce I_{LL} to an acceptable value by imposing a limit value for C_{P2}, as given

by (12). If a dual-parallel-capacitor configuration is selected the following step is to evaluate C_{P1} in order to verify also the compliance with the I_{LH} current limits. A simple way to perform this analysis is to simplify the circuit shown in Figure 6.a employing the Thévenin's theorem between points *a* and *b*. Figure 6.b shows the simplified circuit. It can be easily observed that $\underline{I}_{LH} = \underline{I}_{Th}$, and therefore the modulus of $\underline{I}_{LH}$ and $\underline{I}_{LL}$ can be determined as a function of C_{P1} using (13) and (14), respectively.

$$\left|\underline{I}_{LH}(C_{P1})\right| = \left|\underline{I}_{Th}(C_{P1})\right| = \frac{\left|\underline{V}_{Th}(C_{P1})\right|}{\left|\underline{Z}_{Th}(C_{P1}) + \underline{Z}_o\right|} \tag{13}$$

$$\left|\underline{I}_{LL}(C_{P1})\right| = \left|\underline{I}_{LH}(C_{P1}) \cdot \frac{R_{lamp}}{R_{lamp} + r_e + \underline{Z}_{C_{P2}}}\right| \tag{14}$$

Where: $\underline{Z}_o$ is the load impedance, obtained by the combination of the lamp resistance, electrode resistance and C_{P2} impedance; $\underline{V}_{Th}$, and $\underline{Z}_{Th}$ are the Thévenin's equivalent voltage and impedance. These quantities can be defined as in (15), (16), and (17).

$$\underline{Z}_o = \frac{\left(\underline{Z}_{C_{P2}} + r_e\right) \cdot R_{lamp}}{\underline{Z}_{C_{P2}} + r_e + R_{lamp}} + r_e \tag{15}$$

$$\underline{V}_{Th}(C_{P1}) = \frac{\underline{Z}_{C_{P1}}}{\underline{Z}_L + \underline{Z}_{C_b} + \underline{Z}_{C_{P1}}} \cdot V_{rms1} \tag{16}$$

$$\underline{Z}_{Th}(C_{P1}) = \frac{\left(\underline{Z}_{L_{ac}} + \underline{Z}_{C_b}\right)}{\underline{Z}_{L_{ac}} + \underline{Z}_{C_b} + \underline{Z}_{C_{P1}}} \cdot \underline{Z}_{C_{P1}} \tag{17}$$

Where: $\underline{Z}_{L_{ac}} = j\omega L_{ac}$; $\underline{Z}_{C_b} = {}^{1}/_{j\omega C_b}$; $\underline{Z}_{C_{P1}} = {}^{1}/_{j\omega C_{P1}}$; $\underline{Z}_{C_{P2}} = {}^{1}/_{j\omega C_{P2}}$. Finally the total impedance of the circuit may be defined as $\underline{Z} = \underline{Z}_{Th} + \underline{Z}_o$.

Figure 7 shows the plots of the I_{LL} and I_{LH} rms values as a function of C_{P1} for the T5 HE 35W lamp and the current limits imposed by the IEC 60081.

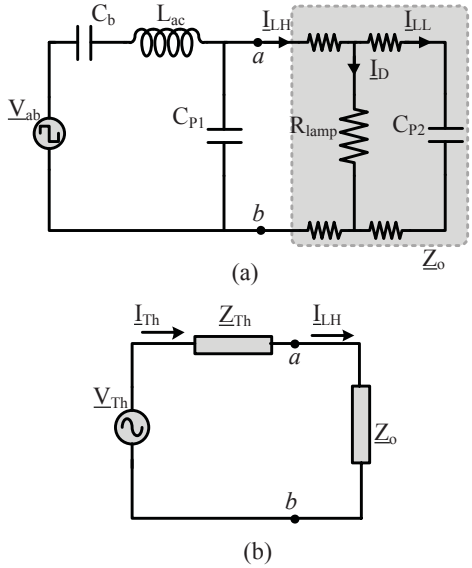

Fig. 6. Equivalent circuit schematic: (a) Modified; (b) Thévenin's equivalent circuit.

The lower minimum values for I_{LL} and I_{LH} are determined by the T5 HE series, however, as previously referred, the T5 HE 35W presents the highest lamp voltage and at the same time the lowest discharge current. As a result, this lamp presents the worst limiting conditions from the set of the selected T5 lamps.

Nonetheless, it is noticed that these minimum values are merely referred by accuracy, since they would only be relevant for dimming operation, particularly for low power dimming levels. It is recalled that this multi-Watt MCEB is only expected to operate all lamps at their nominal power.

So, the plot in Figure 7 assumes C_{p2} at the previously determined value, 2.2nF, R_{lamp} at the rated values of voltage and current for 35W lamp, L_{ac} as calculated in (7) and C_b at 1μF.

The plot shows that any value of C_{P1} may be employed without exceeding the limits of I_{LL} and I_{LH} defined by the dotted lines. Thus, an ideal value of C_{P1} may be selected, around 2.2nF, in order to obtain an equivalent capacitance $C_{Peq} = C_{P1} + C_{P2}$, near 4.7nF, which corresponds to the ideal capacitance defined in the traditional design methodology.

3) Quality factor analysis and ZVS operation - Experimental tests performed in the laboratory shown a proper operation of all lamps at nominal power except for the HE 35 W lamp, for which power oscillations were observed using the selected set of C_{P1} and C_{P2}.

The analysis of the lamp oscillations imply the analysis of the quality factor, Q, of the filter, considering each T5 FL using the predetermined resonant parameters. Table III shows the value of Q and the damping factor, ζ, obtained using (3) and (18), as well as the resonant frequency and the phase ϕ of the circuit's impedance.

$$\zeta = \frac{1}{2Q} \tag{18}$$

Table III reveals that the T5 HE 35W lamp has the lowest ζ and the highest Q values which may be considered as the cause for the FL oscillations. In order to avoid these oscillations, ζ should be increased, which can be done by selecting a lower value of C_{P1}. As result from the previous observation, a C_{P1} =1.1nF was selected and new tests were performed.

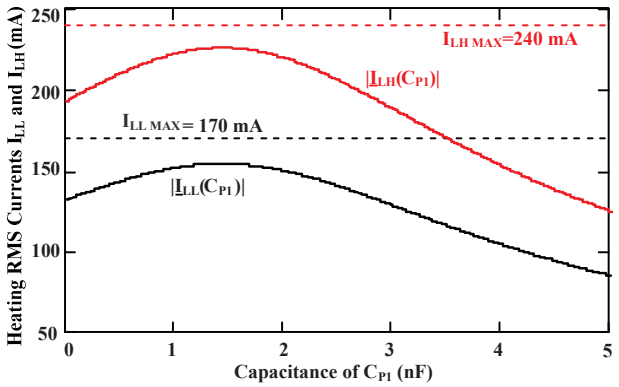

Fig. 7. Selection of C_{P1} versus I_{LH} and I_{LL} limits for FL T5HE35W.

TABLE III
Quality and Damping Factor Q and ζ for C_P = 4.4nF and Q_1 and ζ_1 for C_P = 3.3nF

Lamp	Q	ζ	f_r [kHz]	$\phi[^0]$	Q_1	ζ_1	f_{r1} [kHz]	$\phi_1[^0]$
HE 14 W	0.66	0.76	-	60.9	0.57	0.88	-	66.1
HE 21 W	0.99	0.51	-	54.6	0.85	0.59	-	56.7
HE 28 W	1.36	0.37	33.6	51.1	1.18	0.42	30.4	48.0
HE 35 W	1.71	0.29	40.1	49.7	1.48	0.34	42.1	41.1
HO 24 W	0.43	1.17	-	59.1	0.37	1.35	-	63.9
HO 39 W	0.62	0.80	-	45.7	0.54	0.93	-	51.6
HO 49 W	1.26	0.40	37.5	29.9	1.09	0.46	28.7	32.3

The new values of Q and ζ named as Q_1 and ζ_1 are shown in Table III. Assuming this new C_{P1}, value the equivalent capacitance C_P is now equal to 3.3nF. Experimental results will be presented in section IV indicating that no lamp power oscillations were observed for the critical lamp with this set of parameters.

Table III both show Q and Q_1 values higher and smaller than 1. When Q or $Q_1 < 1$, the traditional concept used to characterized the half-bridge switching conditions cannot be applied, since there will be no corresponding resonant frequency to be shown in Table III. Therefore, using the traditional method, only for a quality factor $Q \geq 1$ it is possible to apply the resonant frequency concept, which immediately guarantees ZVS operation. It is therefore expected that the following lamps, the HE 28W, the HE 35W and the HO 49W will operate in a resonant mode and the resonant current will present in these conditions a near sinusoidal waveform. Although for some set of components this concept is not applicable, we can observe that for all cases the phase ϕ of the circuit's impedance is always positive. Therefore, the circuit will maintain an inductive characteristic whether it operates in a resonant mode or not. These observations are valid for both Table III and Table IV.

Figure 8 show the frequency response for the 35W FL in terms of lamp power and phase angle of the circuit's impedance: $P_{lamp}(R(P), f_s)$, and $\phi(Z(R(P), f_s)$ for C_{Peq} = 3.3nF. Figure 8 shows also that any phase angle is positive around the electronic ballast f_s. Therefore, an increase in the operating frequency will not affect ZVS operation, since will be operating above the resonant frequency. Figure 9 shows the effect of a possible inductance variation on the lamp power for the selected FLs using each corresponding $R_{lamp}(P)$ curve, previously retrieved from the experimental HF characteristics (using commercial electronic ballasts).

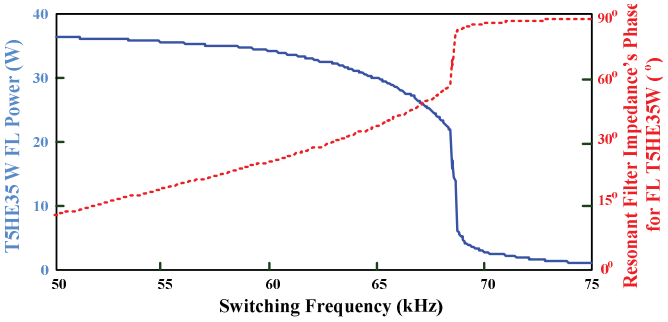

Fig. 8. Phase of circuit's impedance and lamp power using the fluorescent-lamp model versus frequency for T5 HE 35W lamp.

For each FL it is also possible to compare the lamp power curve with the predicted operating point. It is pointed out that in (9) the lamp's electrodes are neglected, therefore $R_{lamp} \cong R_{arc}$, implying that $P \cong P_{arc}$.

Therefore, for future comparison with multi-Watt MCEB experimental results it is preferred to use the experimental high-frequency characteristic $R_{arc}[P_{arc}]$ easily obtained using commercial ballasts.

4) Design Procedure - Figure 10 summarizes the design procedure proposed in this paper. It starts by defining the dc bus voltage, V_{dc}, the operating frequency, f_s, calculating V_{rms1}, selecting the first lamp and collecting its nominal characteristics, then calculate Z_b, L_{ac} and C_P. The same process is repeated until all lamps are considered. These values of L_{ac} and C_P represent the initial pre-set values. The next step is to determine the group of C_P values defined by the SoS limits, according to (12). The flowchart shows that the final C_P value is determined by $C_P = min[C_{P_i}]$; i=1,…,n. This minimum value is given by the lamp with the lowest I_{LLmax} and the highest V_{lamp}. If this value is sufficient to guarantee that all lamps are ignited, the ballast is tested using these parameters. If not, the dual-parallel configuration is adopted, C_{P2} is set equal to the previously determined C_P. The selection of C_{P1} is done using the restrictions given by $I_{LL}(C_{P1}) < I_{LLmax}$ and $I_{LH}(C_{P1}) < I_{LHmax}$ using (13) and (14).

The phase of $\underline{Z}$ is determined in order to verify ZVS and Q and ζ are calculated. The ballast is then tested with all the lamps. For the single or dual-parallel capacitor configurations, if lamp power oscillations are experimentally observed some steps are added to the process: decrease the value of C_{P1} in order to decrease the quality factor Q of the load and therefore increase the damping factor ζ of the circuit.

If the design procedure is applied to the lamps hereby selected, it is possible to conclude that the single parallel capacitor configuration would lead to excessive current into the electrodes and this would contribute to their quick degradation over time. Therefore, the solution is to adopt a dual-parallel-capacitor configuration and by doing so, guaranteeing compliance with the current standards.

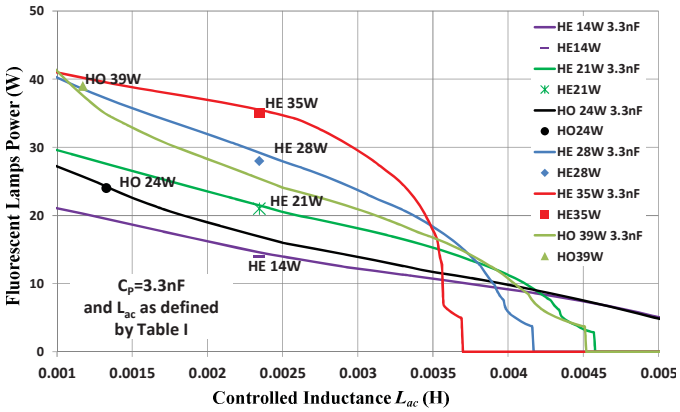

Fig. 9. Inductance L_{ac} variation and its effect on the lamp power considering C_{Peq} = 3.3nF.

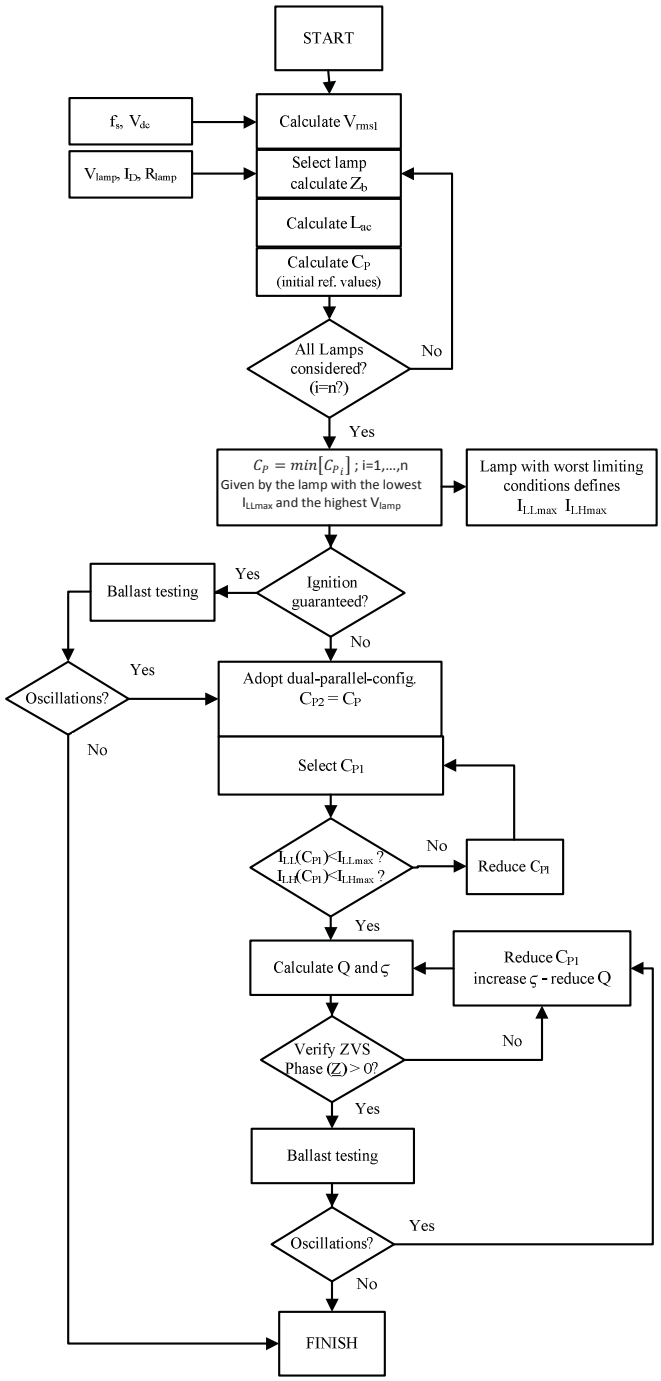

Fig. 10. Multi-Watt MCEB design methodology: flowchart.

C. Inductance: Variable Inductor

The design of the magnetic regulator must be done considering a quite broad inductance range, in order to cover all calculated inductance values. According to the values presented in Table I, the magnetic regulator must have as a minimum, an inductance variation between 1mH and 2.5mH, approximately. The magnetic regulator can be implemented using a gapped E or EFD core set. The main ac winding, which corresponds to the variable inductance responsible for the power control, is placed in the middle leg of the core and the control windings are placed in the left and right legs, in opposite polarity [1]-[4]. An experimental prototype was built using two EFD20/10/7 cores, with N87 type core material. The prototype and the small-signal characteristic of the magnetic regulator, for a dc control current of 0 to 1A, are both presented in Figure 11. The main winding, N_{ac} is composed of 150 turns while the control windings, N_{dc} is equal to 55 turns. The gap g in the main winding is 0.25mm. The small-signal characteristic was obtained using a LCR meter. The maximum inductance value is obtained for a zero dc current value.

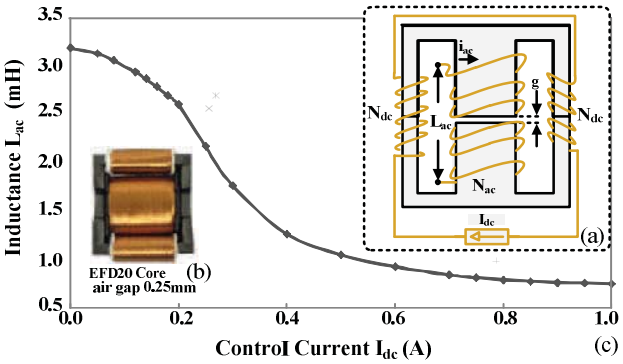

Fig. 11. Variable inductor: (a) Schematic: core, winding, and auxiliary windings; (b) Experimental prototype; (c) Small-signal characteristic.

IV. EXPERIMENTAL RESULTS

A. Experimental Prototype

A digitally-controlled multi-Watt MCEB was developed and an experimental prototype was built according to the schematic shown in Figure 12, considering the design procedure described in the previous sections. Each T5 FLs is therefore supplied by a voltage-fed resonant inverter connected to a parallel-loaded resonant circuit. The ballast requires two additional dc-dc converters, one specifically for the control of the magnetic regulator, and a microcontroller unit, μC. The magnetic regulator is controlled by a dc-dc buck converter operating in CCM. The inductance variation is imposed by the output dc current, I_{dc}, of this converter, which is directly connected to the control windings of the regulator. The control of I_{dc} itself, is done by adjusting the duty-cycle of a PWM signal generated by the μC, and applied to converter, according to a voltage reference, V_{ref}.

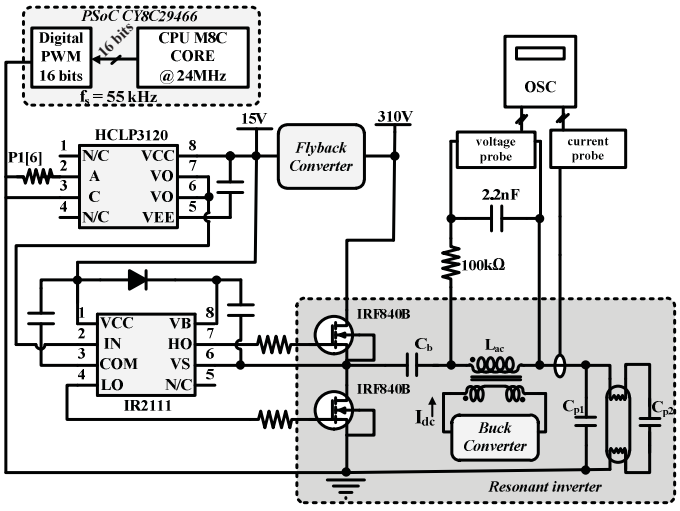

Fig. 12. Digitally-controlled multi-Watt MCEB schematic.

This voltage reference may be imposed manually, or by the μC according to the implemented lamp detection method. The voltage required for the gate driver and the buck converter, 15V, is generated by a dc-dc flyback converter, powered by the ballast dc bus voltage, V_{dc}. The flyback converter will also ensure electrical isolation between the power stage and the control stage of the ballast. This isolation is also guaranteed by two additional optocouplers, one used in the dc-dc buck converter and the other in the gate driver. At last, the gate driver, responsible for setting the inverter switching frequency, f_s, is also managed by the μC, during the preheating mode and at steady-state conditions. As usual, the generated PWM signal will have a duty-cycle of approximately 50%, for an even aging of the lamp electrodes.

B. Experimental Data Analysis

The data collected during prototype testing were obtained with a Picoscope. The first step is to adjust the ballast initial settings, $f_s = 55$ kHz, $V_{dc} = 310$ V and $I_{dc} = 0$. Afterwards, I_{dc} is increased in order to ignite the attached lamp: the inductance value is lowered by adjusting the buck converter duty-cycle until ignition is obtained.

Finally, the regulator's inductance is adjusted until both rms values of lamp voltage and arc current are coherent with the values imposed by the manufacturer. Collected data, presented in Table IV, shows adequate and safe operation for all T5 FLs. Table IV shows the obtained values for all lamps in terms of V_{lamp}, I_D, heating currents, I_{LH}, and I_{LL}. It can be seen that for almost all selected lamps, the rms values of I_{LH} and I_{LL} are below or within the maximum admissible limits.

TABLE IV
Power Rating of the Electronic Ballast and T5 Lamps

Lamp	I_{LL} [mA]	I_{LH} [mA]	V_{EL} [V]	P_{LA} [W]	P_{ARC} [W]	P_{EL} [W]	V_{LA} (V)	I_D (mA)	η [%]
HE14W	77	168	2.46	14.0	13.98	0.72	88.0	161	81.2
HE21W	108	202	3.50	21.4	21.09	1.22	129.2	166	90.5
HE28W	141	221	5.26	28.8	27.99	2.09	175.6	162	92.7
HE35W	181	238	6.29	36.0	34.65	2.74	219.5	160	94.2
HO24W	72	326	0.86	24.1	24.21	0.45	79.6	306	85.1
HO39W	105	349	0.95	38.7	38.95	0.44	122.9	319	87.2
HO49W	175	274	1.17	44.0	43.2	1.17	223.7	195	91.6

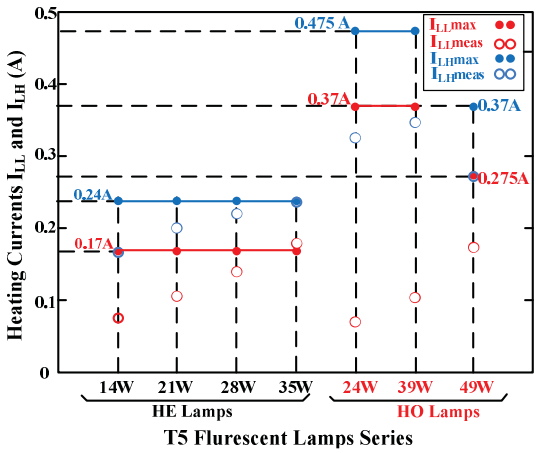

Fig. 13. Experimental results of heating rms currents for all tested T5 FLs.

There is only one limit case: the T5 HE 35W lamp presented an I_{LL} value 6% higher than the permitted value. However, this percentage is acceptable considering the features of the proposed universal electronic ballast that limit the design to attend almost all of T5 fluorescent lamps. It also shows the measured electrode voltage, V_{electr}, and the average lamp power, P_{lamp}. The lamp power is given by the dc average value of the product between the lamp voltage and I_{LH}. Heating currents I_{LH} and I_{LL} show satisfactory results when compared to the maximum limits, previously presented in Table II. Figure 13 shows a graphic view of I_{LH} and I_{LL} for all T5 lamps. It is possible then to compare the measured experimental values with the maximum limits for each lamp series. The overall efficiency of the prototype with each lamp rounds about 89%, which is fairly acceptable for a universal EB. It is however pointed out that this topology does not include a PFC stage. A small decrease of this efficiency should be expected if this stage was included. Using a PFC boost converter operating in critical conduction mode a efficiency of 95% could be achieved for the PFC. Then, the total estimated efficiency of the complete ballast would be around 85%. Except for the T5 HO 49 W all the lamps are operated at rated lamp power and all the minimum values for the discharge current, I_{Dmin}, are fulfilled. The T5 HO 49 W is however operated at a value slightly lower than the minimum limit recommended by the manufacturer.

In order to verify if the lamps present a normal operating condition at steady-state, the lamp operating waveforms were also measured. Figure 14 show the waveforms of the electrodes voltage v_{electr}, the heating currents i_{LL}, and i_{LH}, and the resulting discharge current i_D that is composed by both heating currents i_{LL}, and i_{LH}, for all FLs. It is clear that not all corresponding waveforms present similar shapes, mainly v_{electr} and i_{LL}. Nevertheless all current waveforms present rms values within current standards. Thus, the electrodes temperature is kept within the stipulated limits. According to the manufacture's recommendation, this condition is enough to guarantee the lifetime of the electrodes. In conclusion, the proposed design procedure and the MCB operation, both guarantee a standard lifetime for all selected T5 FLs.

Figure 15 shows the reference value of the lamp power for each FLs and the difference between the experimental operating point for the FLs and the initial theoretical operating point in terms of lamp power and inductance. This slightly different behaviour was expected. The method that was used for determining the resonant circuit parameters is based on the fundamental approximation and the equations are defined assuming that the circuit is operating near resonance. However as discussed previously some of the sets of fluorescent lamp plus filter circuit are not in resonant mode and in those circumstances the resonant current will not assume a perfect sinusoidal waveform. Figure 15 also shows the theoretical values of the lamp power as function of the experimental inductance values using (9). Again similar observations can be made. This implies that the real inductance value required to operate each lamp at its rated power is as expected slightly different.

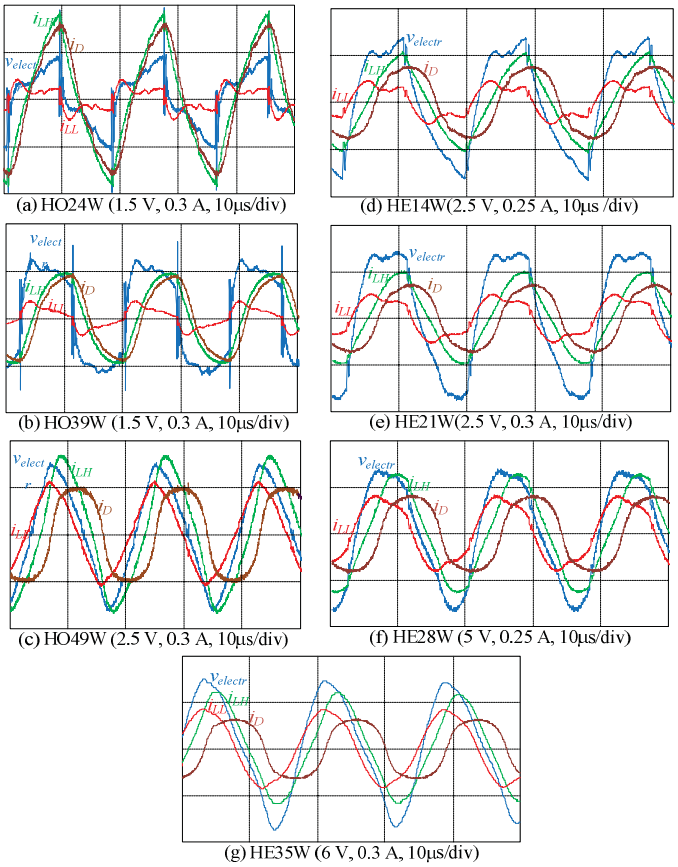

Fig. 14. Experimental waveforms for electrodes voltage v_{electr}, heating currents i_{LH}, i_{LL}, and discharge current i_D:(a), (b), (c) for T5 HO lamp series and, (d), (e), (f) and (g) for T5 HE lamp series.

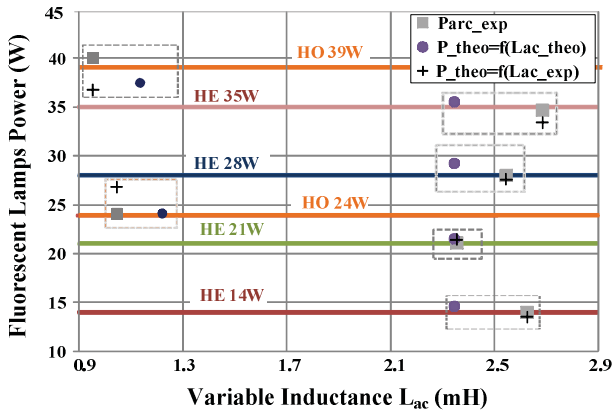

Fig. 15. Operating points for the HE 14W-35W and HO 24W-39W: Lamp power as function of the inductance value for C_p=3.3nF.

V. CONCLUSION

This paper proposes a design methodology suitable for multi-Watt T5 electronic ballasts, based on magnetic control. Stable lamp operation was obtained through a suitable design procedure which ensures the fulfilment of the HE-HO T5 lamps operation limits. Specifically, it proposes a design methodology for the estimation of the resonant circuit parameters, based on the *SoS* technique and the IEC 60081 standard. This technique is based on the observation of the electrodes currents, setting safe operational limits for these currents, for each rated lamp power. All the lamps were operated at a constant frequency, avoiding concerns related to EMI and switching losses. Using the dual-parallel-capacitor configuration, all T5 FLs were operated within the values recommended for nominal lamp operation, ZVS was also ensured, and the electrodes' currents were kept within recommended limits. The proposed design methodology discloses the necessity to fulfil current regulations in order to maintain the manufacturers estimated lamp life. It represents an efficient alternative to enhance the performance of multi-Watt T5 MCEB. This procedure can be extended to other EB, since most of FLs ballasts are typically parallel-loaded half-bridge based inverter circuits. It can also be adapted to dimmable systems. In dimming operation, instead of having one limit *SoS* value for the electrode currents, maximum, minimum and target *SoS* curves are defined for the whole dimming range. It is also pointed out that in this multi-Watt MCEB no external heating sources are used and therefore the cost-penalty of including this type of electrode operation control is avoided.

ACKNOWLEDGEMENT

This work was co-sponsored by the Spanish Government, Education and Science Office, under research grant number DPI2007-61267 and DPI2010-15889, and by the Government of the Portuguese Republic, FCT-MCTES, under research grants numbers PTDC/EEA-ENE/66859/2006 and SFRH/BD/36143/2007.

REFERENCES

[1] M. S. Perdigão, J. M Alonso, D. G. Vaquero, and E. S. Saraiva, "Magnetically-Controlled Electronic Ballasts with Isolated Output: The Variable Transformer Solution", *IEEE Transactions on Industrial Electronics*, vol. 58, no. 9, pp. 4117-4129, September 2011.

[2] J. M. Alonso, M. S. Perdigão, J. Ribas, D. Gacio Vaquero, and E. S. Saraiva, "Optimizing Universal Ballasts Using Magnetic Regulators and Digital Control", *IEEE Transactions on Industrial Electronics*, vol. 58, no. 7, pp. 2860-2871, July 2011.

[3] M. S. Perdigão, J. M. Alonso, M. A. Dalla Costa, and E. S. Saraiva, "Comparative Analysis and Experiments of Resonant Tanks for Magnetically Controlled Electronic Ballasts", *IEEE Transactions on Industrial Electronics*, vol. 55, no. 9, pp. 3201-3211, September 2008.

[4] M. S. Perdigão, J. M. Alonso, M. A. Dalla Costa, and E. S. Saraiva, "Using Magnetic Regulators for the Optimization of Universal Ballasts", *IEEE Transactions on Power Electronics*, vol. 23, no. 6, pp. 3126-3134, November 2008.

[5] U. Boeke, "Scalable Fluorescent Lamp Driver Using Magnetic Amplifiers", *in Proc. of ECCE,* 2005.

[6] Y. Hu, L. Huber, and M. Jovanovic, "Single-Stage, Universal-Input AC/DC LED Driver with Current-Controlled Variable PFC Boost Inductor", *IEEE Transactions on Power Electronics*, vol. 27, no. 3, 1579- 1588, March 2012.

[7] A. A. Huzayyin, "Utilizing the Nonlinearity of a Magnetic Core Inductor as a Source of Variable Reactive Power Compensation in Electric Power Systems", *in Proc. IEEE AISPC*, pp 1-4, 2008.

[8] H. I. Sewel1, D. A. Stone, and D. Howe, "Dynamic Load Impedance Correction for Induction Heaters", *in Proc. IEEE PEDS*, vol 01., pp. 110-115, 1999.

[9] J. M. Alonso, M. S. Perdigao, D. Gacio, L. Campa, and E.S. Saraiva, "Magnetic control of DC-DC resonant converters Provides Constant Frequency Operation", *Electronics Letters*, vol. 46, no. 6, pp. 440-442, March 2010.

[10] *Philips MASTER TL5 lamps, Philips 2006*. (2011). Available: http://www.lighting.philips.com.

[11] R. Casanueva, C. Brañas, Francisco J. Azcondo, and F. Javier Díaz, "Teaching Resonant Converters: Properties and Applications for Variable Loads", *IEEE Transactions on Industrial Electronics*, vol. 57, no. 10, pp. 3355-3363, October 2010.

[12] C. Ekkaravarodome, A. Nathakaranakule, and I. Boonyaroonate, "Single-Stage Electronic Ballast Using Class-DE Low-dv/dt Current-Source-Driven Rectifier for Power-Factor Correction", *IEEE Transactions on Industrial Electronics*, vol. 57, no. 10, pp. 3405-3414, October 2010.

[13] J. Lopes, M. A Dalla Costa, F. E Bisogno, R. N. Prado, and A R.Seidel, "Feedforward Regulation Method for Self-Oscillating Electronic Ballast for Fluorescent Lamps," *IEEE Transactions on Industrial Electronics,* vol. 59, no. 4, pp. 1869-1878, April 2012.

[14] J. M. Alonso, Electronic Ballasts in M. H. Rashid (Eds), *Power Electronics Handbook*, San Diego: Academic Press, pp. 565-590, 2001.

[15] M. K. Kazimierczuk, D. Czarkowski, *Resonant Power Converters*, Ed. John Wiley & Sons, 1995, pp 201-239.

[16] J. Ribas, J. M. Alonso, E. L. Corominas, A. J. Calleja, M. Rico-Secades, "Design Considerations for Optimum Ignition and Dimming of Fluorescent Lamps Using a Resonant Inverter Operating Open Loop", *in Proc. IEEE IAS*, pp. 2068-2075, 1998.

[17] M. K. Kazimierczuk, W. Szaraniek, "Electronic Ballast for Fluorescent Lamps," *IEEE Transactions on Power Electronics*, vol. 8, no. 4, pp. 386-395, October 1993.

[18] U. Mader "Steady-state Analysis of a Voltage-fed Inverter with Second-order Network and Fluorescent Lamp Load", *in Proc. IEEE APEC*, pp. 609-615, 1996.

[19] Z. Li, P. K. T. Mok, W. H. Ki, and J. K. O. Sin, "A Simple Method to Design Resonant Circuits of Electronic Ballast for Fluorescent Lamps", *in Proc. IEEE ISCAS*, pp. 1744-1747, 1997.

[20] T. J. Ribarich, J. J. Ribarich, "A New Procedure for High Frequency Electronic Ballast Design", *IEEE Transactions on Industry Applications*, vol. 37, no.1, pp. 262-267, January/February 2001.

[21] R. N. Do Prado, A. R. Seidel, F. E. Bisogno, M. A. D. Costa, "A Design Method for Electronic Ballast for Fluorescent Lamps", *in Proc. IEEE IECON*, pp. 2279-2284, 2000.

[22] T, J. Liang, C. A. Cheng, W. B. Shyu, J. F. Chen, "Design Procedure for Resonant Components of Fluorescent Lamps Electronic Ballast Based on Lamp Model", *in IEEE PEDS*, pp. 618-622, 2001.

[23] C. S. Moo, H. L. Cheng, H. N. Chen, H. C. Yen, "Designing Dimmable Electronic Ballast with Frequency Control", *in Proc. IEEE APEC*, pp. 727-733, 1999.

[24] C. S, Moo, H. L. Cheng, Y. N. Chang, "Single-stage High-power Factor Dimmable Electronic Ballast with Asymmetrical Pulse-width Modulation for Fluorescent Lamps," *IEE Proc. of Electric Power Applications*, vol. 148, no. 2, pp. 125-132, March 2001.

[25] F. E. Bisogno, Á. R. Seidel, R. Holsbach, R. N. do Prado, "Resonant Filter Applications in Electronic Ballast", *in Proc. IEEE IAS*, pp. 348- 354, 2002.

[26] Á. R. Seidel, F. E. Bisogno, R. C. D. de Paiva, and R. N. do Prado, "Analysis of the LCC Resonant Filter Used in Fluorescent Systems Considering the Filaments", *in Proc. COBEP*, 2003.

[27] F. T. Wakabayashi, C. A. Canesin, "An improved Design Procedure for LCC Resonant Filter of Dimmable Electronic Ballasts for Fluorescent Lamps, Based on Lamp Model", *IEEE Transactions on Power Electronics*, vol. 20, no.5, pp. 1186- 1196, September 2005.

[28] F. T. Wakabayashi, M. A. Gomes de Brito, C. S. Ferreira, C. A. Canesin, "Setting the Preheating and Steady-State Operation of Electronic Ballasts, Considering Electrodes of Hot-Cathode Fluorescent Lamps", *IEEE Transactions on Power Electronics*, vol. 22, no.3, pp. 899-911, May 2007.

[29] M. Polonskii, R. A. Eichelberger, T. M. Rodegheri, J. C. A. Rigo, and Á. R. Seidel, "Designing Dimmable Electronic Ballasts with Frequency Control", *in Proc. COBEP*, 2007.

[30] G. Spiazzi and S. Buso, "Non-Iterative Design Procedure of LCC-based Electronic Ballasts for Fluorescent Lamps Including Dimming Operation", *in Proc. IEEE ECCE*, 2009.

[31] J. Ribas, R.E. Díaz, A.J. Calleja, E.L. Corominas, J. García, "Electrode Characterization in Dimmed Operation of Fluorescent Lamps", *in Proc. IEEE IECON*, p. 2559 – 2564, 2010.

[32] IEC60081. Double-capped fluorescent lamps. Performance specifications. 2010.

[33] GE Lighting, T5 Long Last, Linear Fluorescent Lamps, Datasheet. (2009). Available: http://www.gelighting.com/eu/resources/literature_library/prod_tech_pub/downloads/t5_data_sheet.pdf.

[34] W. M. Ng, D. Y. Lin, and S. Y. Hui, "Design of a Single Ultra-Low-Loss Magnetic Ballast for a Wide Range of T5 High-Efficiency Fluorescent Lamps", *IEEE Transactions Industrial Electronics*, vol. 59, no. 4, pp. 1849-1858, April 2012.

[35] International Electrotechnical Commission. *Ballasts for tubular fluorescent lamps - Performance requirements*, IEC 60921, 2006.

[36] International Electrotechnical Commission. *AC supplied electronic ballasts for tubular fluorescent lamps - Performance requirements*, IEC 60929, 2006.

[37] D. M. Buso, M. Mayrhofer, S. Zudrell-Koch, M. Severinsson, and G. Zissis, "Influence of Auxiliary Heating on the Degradation of Fluorescent Lamp Electrodes Under Dimming Operation", *IEEE*

Transactions Industrial Electronics, vol. 59, no. 4, pp-. 1889-1897, April 2012.
[38] R. Gules, W. M. dos Santos, E. R. Romaneli, C. Q. Andrea, and R. Annunziato, "An Auxiliary Self-Oscillating Preheating System for Self-Oscillating Fluorescent Lamp Electronic Ballasts", *IEEE Transactions Industrial Electronics*, vol. 59, no. 4, 1859-1868, April 2012.
[39] L. H Goud and J.W.F. Dorleijn, "Standardized Data for Dimming of Fluorescent Lamps", *in Proc. IEEE IAS,* vol. 1, pp. 673- 679, 2002.
[40] J. W. F Dorleijn, and L. H Goud, "Standardisation of the Static Resistances of Fluorescent Lamp Cathodes and New Data for Preheating", *in Proc. IEEE IAS*, vol. 1, pp. 665- 672, 2002.
[41] D. Lin, W Yan, and S. Y. R. Hui, "Modeling of Dimmable Fluorescent Lamp Including the Tube Temperature Effects", *IEEE Transactions on Industrial Electronics*, vol. 58, no. 9, pp. 4145-4152, September 2011.

BIOGRAPHIES

H. V. Marques was born in Avelar, Portugal, in 1983. He received the M.Sc. degree in electrical engineering from the University of Coimbra, Coimbra, Portugal, in 2010.

Since 2010, he has been a Researcher at the Instituto de Telecomunicacões, Universidade de Coimbra. His research interests include high-frequency electronic ballasts, high-frequency switching converters, resonant converters, power electronics, microcontrollers, and computer simulation applications.

Alysson R. Seidel was born in São Pedro do Sul, Brazil, in 1975. He received the B.S. and Ph.D. degrees in electrical engineering from the Federal University of Santa Maria, Santa Maria, Brazil, in 1999 and 2004, respectively. From 2004 to 2008, he was an Associate Professor in the Department of Electrical Engineering, University of Passo Fundo, Passo Fundo, Brazil. He is currently at the Federal University of Santa Maria, where he has been a Professor at the Colégio Técnico Industrial de Santa Maria and a Researcher in the Electronic Ballast Research Group since 1997 and the Electrical and Computational Systems Research and Development Group since 2010. His research interests include resonant converters, dimming systems, simulation, discharge lamps, and lighting systems. Dr. Seidel is a member of the SOBRAEP - Brazilian Power Electronics Society, and IEEE.

Marina S. Perdigão was born in Coimbra, Portugal, in 1978. She received the M.Sc. degree in electrical engineering from the University of Coimbra, Coimbra, in 2004. She has been working toward the Ph.D. degree from the University of Coimbra in cooperation with the University of Oviedo, Oviedo, Spain, since 2006. Since 2002, she has been an Assistant Professor in the Department of Electrical Engineering, Superior Institute of Engineering of Coimbra, Coimbra. Since 2001, she has also been a Researcher at the Instituto de Telecomunicações. Coimbra. Her research interests include high-frequency electronic ballasts, discharge lamp modeling, high-frequency switching converters, resonant converters, power electronics for renewable energies, and computer simulation applications. Dra. Perdigão received the Best Paper Award of the 2009 IEEE International Symposium on Industrial Electronics. She also collaborates as an IEEE Transactions Paper Reviewer.

J. Marcos Alonso received the M.Sc. Degree and Ph.D. both in electrical engineering from the University of Oviedo, Spain, in 1990 and 1994 respectively. Since 2007, he has been appointed as full Professor at the Electrical Engineering Department of the University of Oviedo.

Prof. Alonso is co-author of more than three hundred journal and conference publications. His research interests include electronic ballasts, LED power supplies, power factor correction and switching converters in general. He was supervisor of seven Ph.D. Thesis and he is the holder of seven Spanish patents.

Prof. Alonso has been awarded with the Early Career Award of the IEEE Industrial Electronics Society in 2006. He also holds three IEEE paper awards. Since October 2002 he serves as an Associate Editor of the IEEE Transactions on Power Electronics. He has been Co-Guest Editor of two special issues in lighting applications published in the IEEE Transactions on Power Electronics (2007) and IEEE Transactions on Industrial Electronics (2012) and has co-organized several conference special sessions. He is also member of the European Power Electronics Association and he belongs to the International Steering Committee of the European Conference on Power Electronics and Applications (EPE).

E. Sousa Saraiva received the degree of Electrical Engineer from the University of Oporto, Oporto, Portugal in 1970, and the Ph.D. degree in electrical engineering from the University of London, London, U.K., in 1979. The aggregation in electrical engineering was received from the University of Coimbra, Coimbra, Portugal, in 1985. He served on the Faculty of Science and Technology, University of Coimbra, as an Assistant Eventual from July 13, 1973 to July 12, 1975, as an Assistant from July 13, 1975 to July 24, 1979, as an Auxiliary Professor from July 25, 1979 to November 30, 1979, as an Associated Professor from December 01, 1979 to November 20, 1986, and as a Full Professor from November 21, 1986 to July 31, 2011. He retired on August 1, 2011. He is the coauthor of more than 100 papers in national and international journals and conferences. He was the adviser of 12 postgraduate students, coadviser of another, and currently a coadviser of one Ph.D. student and coadviser of a M.Sc. student. His research interests include electric machines, power electronics, the influence of the electromagnetic field in the human body, and, more recently, electronic ballasts for fluorescent lamps.

Dr. Saraiva has been a member of the IEEE for more than 25 years and collaborates as a Reviewer. He is one of the founders of the IEEE Portugal Section. He is a member of the Portuguese "Ordem dos Engenheiros," having in the past, been elected to positions in the Central Region and on National Boards.